Flexible Radio Frequency Pulse Optimization using Deep Learning Methods

Tristhal Parasram, Dan Xiao
University of Windsor, Windsor, Canada

Introduction:

Finding optimal MR pulses and pulse sequences for specific applications has long been an area of interest. Recently, deep learning has been explored for MR pulse optimization [1-3], demonstrating flexibility in targeting specific pulse characteristics [4]. In this work, we present a flexible pulse optimization framework that leverages modern deep learning methods to tune pulses based on a set of input-output examples. Previously, we optimized a pair of 90° and 180° pulses for a slice selective CPMG. In the current study, an improved framework has been applied to optimize prefocused excitation and refocusing pulses with uniform magnitude response and constant phase across the target bandwidth (BW), as well as delay-focused excitation pulses [5] that rephase after a specific duration. Furthermore, low B1 amplitudes were achieved, potentially requiring minimal or no RF amplification from an external power amplifier.

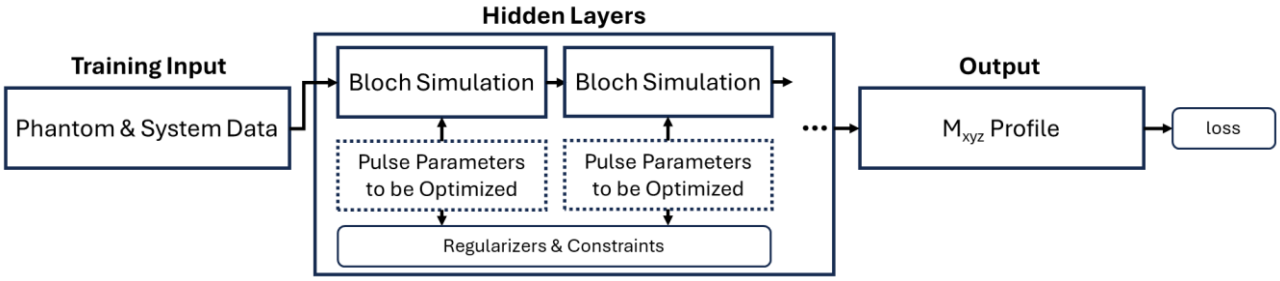

Fig 1. The model structure for RF pulse or pulse sequence optimization. The pulse amplitude, phase and/or gradient are stochastically optimized on batches from a large dataset of simulated phantoms. The dataset describes the desired effect of the pulse through examples of initial conditions and target pulse response. Constraints and regularizers are incorporated into the loss function as additional terms.

Methods:

RF pulses were optimized using a TensorFlow model comprising a trainable pulse parameter layer and a differentiable Bloch simulation layer. The optimization workflow is outlined in Fig. 1. The function of the rf pulse is defined by a dataset of initial conditions and corresponding target responses. The dataset includes system parameters, a sample phantom, and the desired effect of the pulse on the phantom. The model is trained to minimize the difference between the simulated and target responses across a group of phantoms, as specified by the loss function.

$$loss = MAE(\boldsymbol{M_{pulse}}, \boldsymbol{M_{target}}) + \|P_{amp}\|_2 + \|P_{phase}\|_2 + \|P_{grad}\|_2 + R(P) + C(P) \quad (1)$$

The first term is the mean absolute error between the simulated and target responses. The 2nd-4th terms are L2 norms on the pulse parameters, and the last two terms represent any regularizers R and constraint penalties C applied to the pulse.

In this work, the model was trained on 2^{16} simulated phantoms with random frequencies within a 1kHz range, minimizing post-pulse magnetization error relative to 3 target states. The first target is a prefocused excitation that flips equilibrium magnetization purely to M_y. This is paired with a refocusing pulse trained to perform a 180° rotation about the x-axis on randomly oriented M_{xy} with a small z component. Finally, a delay-focused excitation was developed, similar to the prefocused 90° target, but with an added free precession layer following the pulse, causing the magnetization to come into phase a specified time after transmission. To produce practical, low-amplitude RF pulses, L2 regularization and amplitude constraints were applied to the pulse parameters P.

Results and Discussion: A 10 ms prefocused 90° excitation and 180° refocusing pulse (Fig. 2 a,b) were optimized to achieve a uniform M_y flip across a 1 kHz BW. The resulting frequency response profiles for the 90 (Fig. 2c) closely matched the target, without the linear phase observed in a square pulse (Fig. 2e). In the presence of significant B0 inhomogeneity, Mxy phase variation cannot be removed by applying a gradient pulse. The prefocused pulse produces in-phase magnetization immediately after transmission. The optimized 180° refocusing pulse preserves magnetization across the BW without distortion at the echo (Fig. 2d), whereas the rectangular 180° pulse further reduces M_{xy} at higher frequences (Fig. 2f). Overall, the optimized result provides more uniform spectral weighting, minimizing attenuation of high-frequency components.

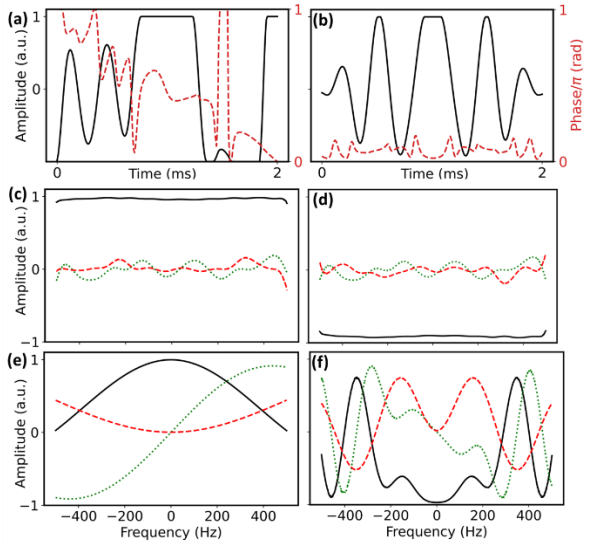

Fig 2. (a) Optimized 90° excitation and (b) 180° refocusing pulses, with amplitude (black) and phase (red dashed). The phase is constrained between 0 and π, and the pulse amplitude is flattened at the top due to the peak amplitude constraint. (c) Simulated magnetization response to the optimized 90° pulse and (d) optimized 180° pulse applied in a spin echo sequence with a 2 ms echo time. (e) Simulated magnetization response to a hard 90° excitation with equal peak amplitude to the optimized pulse, and (f) hard 180° pulse with the same amplitude as the optimized refocusing pulse, also applied in a spin echo. Responses are shown at the echo time. Colors: solid black = M_y, dotted green = M_x, and dashed red = M_z.

Delay-focused 90° pulses were optimized to generate echoes 0.5 ms, 1 ms, and 2.5 ms after transmission. The pulse with a 1 ms delayed focus (Fig. 3a) produced a frequency response similar to Fig. 2c at the echo time. Applied experimentally to an aqueous $CuSO_4$ phantom, it yielded a correctly timed echo (black), compared to a conventional hard-pulse spin echo (red) in Fig. 3b which was delayed by 1 ms. In simulation, a standard sinc pulse produces an echo with a 5 ms delay. The optimized pulse amplitude was 20% higher than a hard 90° pulse but 40% lower than a hard 180° pulse of equivalent BW.

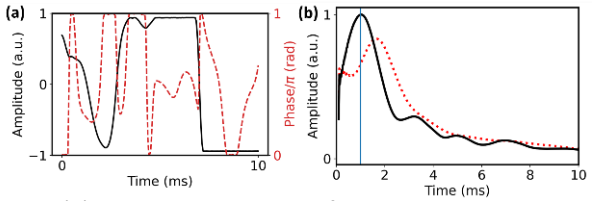

Fig 3. (a) Optimized 90° delay-focused excitation pulse with amplitude (black) and phase (red). (b) Experimental FID signal magnitude after the optimized 90° (black) and a spin echo signal with 2 ms echo time (red) on an aqueous $CuSO_4$ phantom containing titanium metal to increase B0 inhomogeneity. The vertical line marks the target echo time.

When T_2* star is very short, the signal may be lost during the dead time. A delay-focused pulse can overcome this by shifting the point of rephasing beyond the dead time. For example, reducing the pulse duration to 200 us allows an echo delay of 50 us potentially bypassing the probe deadtime.

For a 60 mm, 2MHz solenoid coil, the RF power required to achieve a 1kHz bandwidth is on the order of tens of milliwatts. If only a 100-200 Hz bandwidth is required, the power can be reduced to <1mw, potentially eliminating the need for an external RF amplifier.

Conclusion: A flexible pulse generation framework was developed that requires only initial system conditions and corresponding target responses. The optimized pulses are particularly useful for low-field, low-cost MR systems with greater B0 inhomogeneity, and for systems with short T_2*. The pulses were validated through simulation and experiment. The framework also supports extension for pulse sequence design, incorporating B_0 and B_1^+ maps, power and slew penalties, and more.

References: [1] Loktyushin et. Al, Magn. Reson. Med. (2021). [2] Zhu et. Al Magn. Reson. Med. (2022) [3] Perlman et. Al Magn. Reson. Med. [4] Jang et. Al, Magn. Reson. Med. (2024). [5] Shen, Jour. Magn. Reson. (2001). [6] Parasram et. Al ISMRM (2025)